Progress In Electromagnetics Research C, Vol. 112, 113–125, 2021

Enhanced Ultra-Wide Band Multistage Rectifier for Pulsed Signal Power Transmission

Ahmed Moulay* **and Tarek Djerafi**

Abstract—This paper presents a multi-sections broad-band radio-frequency (RF) to direct-current (dc) power rectifier for pulsed signal transfer. The power transfer using a pulse allows to use a signal with low power spectral density. The optimal distributed configuration with critical parameters is studied to enhance the efficiency over broadband frequency and wide power range. A five-stage distributed RF-dc converter arrangement with micro-strip transmission line ensures the power harvesting from 100 MHz to 11 GHz. The designed and fabricated circuit is characterized at multi-frequencies of ultra-wide band (UWB). The distributed harvester significantly improves the detected voltage over a wide bandwidth compared to conventional RF detectors. The achieved efficiency with optimized parameters is 48% with five-stage harvester. A maximum dc output of 956 mV is reached at 8 dBm of input power of sinusoidal single tone signal at 1 GHz of frequency. The designed prototype is associated with a square wave signal to show the circuit potential in terms of power transfer. The output voltage can be controlled with input signal level, frequency, as well as the pulse width. For the power transfer circuit, 996 mV of maximum dc output voltage is reached for 1 V of input amplitude at 1 GHz with duty cycle of 50%. The efficiency increases significantly with duty cycle ratio of the input signal. The power harvester associated with a UWB antenna confirms the benefit of using a square wave signal in the case of power harvesting or transfer.

1. INTRODUCTION

Wireless power transfer (WPT) and wireless power harvesting (WPH) techniques have recently experienced very rapid growth and interest of researchers. These techniques overcome device powering in internet of things (IoT), as battery use, recharging, and replacement will become cost-prohibitive and non-durable for multiple devices. Meanwhile, with the growing demand for low-power systems such as wireless sensor networks and radio frequency identification (RFID) systems, the energy collection from continuously available RF signals is becoming a luxury extra for these devices. RF energy harvesting from the environment will have an important role in future microelectronic circuits. This concept requires an efficient antenna as well as a circuit capable of converting RF signals to dc voltage, to replace batteries [1–5].

Reported researches on WPH/T show generally optimized performance around one or two bands [6–9]. In [7] using a GaN diode at 5.8 GHz, the dc output power achieved is 200 mW using 0.5 W (27 dBm) of input power which corresponds to 40% of efficiency. This system requires a fairly high input power level (at the antenna level) which is not easy in a real circumstance. A dual-band rectifier with extended power range using PCB process presented in [8] about 50% efficiency is obtained using 7 transmission line segments for a dual-band matching. More elaborated signal should be used to boost the efficiency. The combination of two tones is used in [10] to enhance the RF power harvesting. The WPH in FM

Received 29 March 2021, Accepted 25 April 2021, Scheduled 29 April 2021
* Corresponding author: Ahmed Moulay (ahmed.moulay@inrs.ca).
The authors are with the Department of Energy, Material and Telecommunication, Institut National de la Recherche Scientifique, University of Quebec, Montreal, Quebec, Canada.

broadcast band presented in [10] shows the multi-tone excitation effect on dc output response of the rectifier circuit. In order to achieve high efficiency in the case of power transfer, it is mandatory to send high power which is not authorized by different standards. The low power spectral density can be used in the WPT system to overcome the Federal Communications Commission (FCC) power limit [11]. The pulsed signal naturally contains electromagnetic power over a large frequency bandwidth and can be a practical solution to transfer RF energy. Usually, a UWB signal has a very low power spectral density ($\leq -41\,\mathrm{dBm/Hz}$) [12–14]. Only a few power rectifiers with broad band performance have been reported [15, 16]. These designs have been optimized for the rectification of a single-tone sinusoidal signal in a relatively broad band frequency.

The main objective of this work is to provide a design that maximizes the conversion efficiency between the low-power incident signal and the dc voltage at the receiving load. By using the UWB, we will cover a wide spectrum of ambient communication signals. This increases the presence of frequencies power spectrum to be rectified and overcomes the low-power spectral density of UWB. A UWB rectifier that allows the rectification of different signals is proposed and investigated. This rectifier covers the different wireless power harvesting/transfer (WPH/T) scenarios as shown in Fig. 1. The proposed harvester is capable of handling the presence of one tone, multi-tones, as well as a pulsed signal. This concept allows more RF energy to be harvested at lower density levels. In this scenario, the output voltage level can be controlled not only by the received signal level but also by its periodicity and duty cycle. Theoretical analysis of the square signal rectification based on harmonic tones representation is given in Section 2, to estimate the potential of square pulse. Afterward, in Section 3, the effects of different harvester parameters are studied to enhance the power capability and also efficiency. To validate the theoretical results, the single-tone characterization of manufactured prototype is realized. In Section 4, the UWB power transfer is presented and validated with the experiment showing promising results.

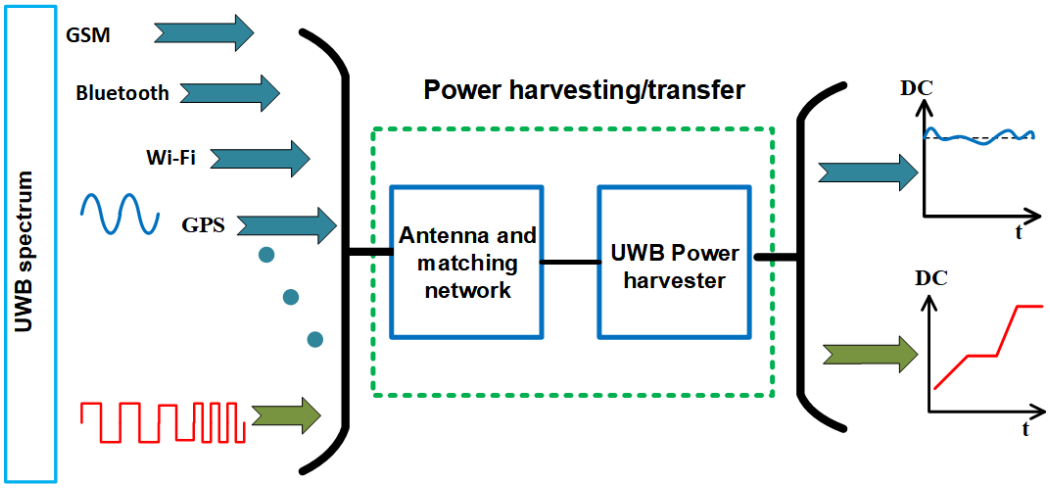

Figure 1. Concept of UWB power harvesting/transfer system.

2. HARMONIC SIGNALS RECTIFICATION

The simple circuit of an RF power detector with zero-bias diode is depicted in Fig. 2. When an RF signal is applied across the diode, it will experience a nonlinear phenomenon. This non-linearity can be represented as a polynomial expansion around the diode operation point [17, 18]. Considering the fourth order to maintain a basic rectification, the approximation of the current flowing through the diode can be written as follows:

$$i_d = I_q + k_1 (v_d - V_q) + k_2 (v_d - V_q)^2 + k_3 (v_d - V_q)^3 + k_4 (v_d - V_q)^4 + \ldots \quad (1)$$

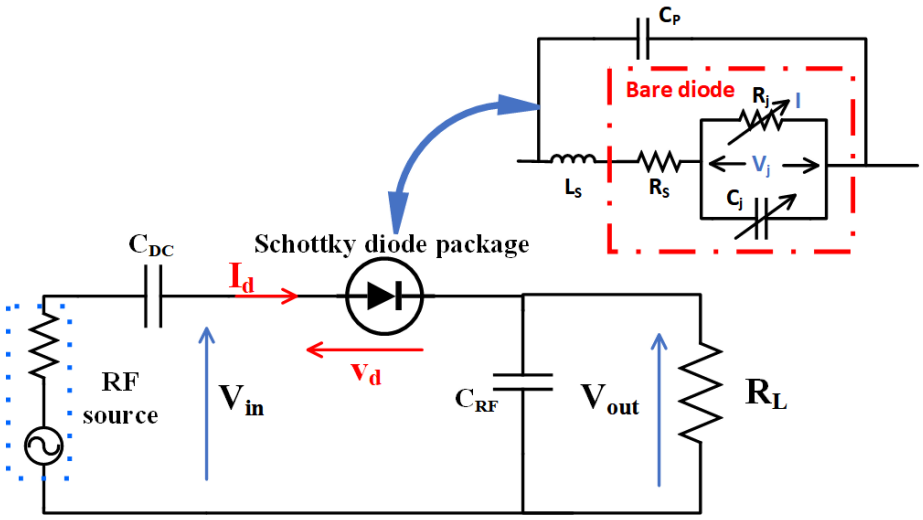

Figure 2. Circuit of RF power detector with zero-bias diode.

where $v_d = V_{in} - V_{out}$ and $k_1, k_2, \ldots, k_n$ are the model coefficients found from the successive derivatives of the diode current [17].

$$k_1 = \frac{1}{1!}\frac{\partial I_d}{\partial V_d}\bigg|_{V_d=V_q};\ k_2 = \frac{1}{2!}\frac{\partial^2 I_d}{\partial V_d^2}\bigg|_{V_d=V_q};\ \ldots;\ k_n = \frac{1}{n!}\frac{\partial^n I_d}{\partial V_d^n}\bigg|_{V_d=V_q} \tag{2}$$

The v_d and i_d signals will be represented by generic signals $x(t)$ and $y(t)$, respectively. Only even order terms will be considered because the odd terms have no effect on the dc component [17, 19].

$$y(t) = k_2 x^2(t) + k_4 x^4(t) \tag{3}$$

Two wave-forms are considered for the RF excitation signal as illustrated in Fig. 3. The following subsections provide a theoretical analysis of two types of input signal: a sinusoidal (first case) and a square wave (second case) in the frequency range of 0.1–11 GHz. For each case, the output signal will be represented by Eq. (3).

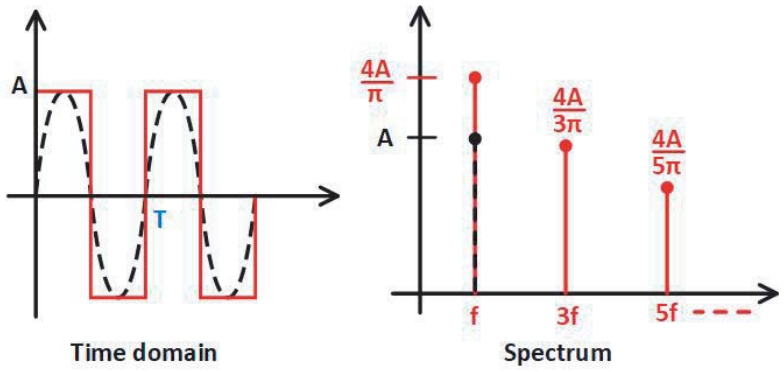

Figure 3. Time and frequency domain of investigated inputs signals.

2.1. Sinusoidal Signal

An RF sinusoidal form of single tone signal with amplitude of B and pulsation of w_1 can be written as:

$$x(t) = B\cos(w_1 t + \varphi_1) \tag{4}$$

Considering Eq. (3), the diode output signal will be:

$$y(t) = \frac{B^2 k_2}{2} + \frac{3B^4 k_4}{8} + \frac{B^2 k_2}{2}\cos(2w_1 t + 2\varphi_1) + B^4 k_4 \cos(2w_1 t + 2\varphi_1) + B^4 k_4 \cos(4w_1 t + 2\varphi_1) \quad (5)$$

Components $2w_1$ and $4w_1$ will be eliminated due to the power harvester behavior [17]. After normalizing the amplitude to 1 (deciding by B), the dc component will be exclusively the remaining terms:

$$y_{dc} = 0.50k_2 + 0.37k_4 \quad (6)$$

As expected, Eq. (6) shows that to maximize the harvested power, the diode must operate in the square-law region where k_2 is the maximum.

2.2. Square Signal

Using Fourier series, we can describe an ideal square signal in an infinite series form:

$$x(t) = \frac{4}{\pi}\sum_{k=0}^{\infty}\frac{\sin((2k+1)2\pi ft)}{(2k+1)} \quad (7)$$

$$x(t) = \frac{4}{\pi}\left(\sin(2\pi ft) + \frac{1}{3}\sin(6\pi ft) + \frac{1}{5}\sin(10\pi ft) + \ldots\right) \quad (8)$$

Considering that the power harvester is excited by a square signal and replaces Eq. (8) in Eq. (3), the diode output becomes:

$$y(t) = k_2\left(\frac{4}{\pi}\left(\sin(2\pi ft) + \frac{1}{3}\sin(6\pi ft) + \frac{1}{5}\sin(10\pi ft)\right)\right)^2 + k_4\left(\frac{4}{\pi}\left(\sin(2\pi ft) + \frac{1}{3}\sin(6\pi ft) + \frac{1}{5}\sin(10\pi ft)\right)\right)^4 \quad (9)$$

The proposed rectifier will cover frequencies up to 11 GHz. Consequently, for square input signal with frequency up to 2.2 GHz (11 GHz/5), the fundamental, 3rd and 5th components should be considered. In this case, the approximated dc component of Eq. (9) is:

$$y_{dc} = 0.93k_2 + 1.24k_4 \quad (10)$$

Hence, for an input signal with frequency between 2.2 and 3.66 GHz (11 GHz/3), only the fundamental and 3rd components are taken into account, and $y(t)$ becomes:

$$y(t) = k_2\left(\frac{4}{\pi}\left(\sin(2\pi ft) + \frac{1}{3}\sin(6\pi ft)\right)\right)^2 + k_4\left(\frac{4}{\pi}\left(\sin(2\pi ft) + \frac{1}{3}\sin(6\pi ft)\right)\right)^4 \quad (11)$$

The intermodulation products greater than 11 GHz will be automatically removed by the power harvester behavior, and the dc output component is:

$$y_{dc} = 0.81k_2 + 0.64k_4 \quad (12)$$

Finally, in the case of square input signal with frequency higher than 3.66 GHz only the fundamental will be considered, and $y(t)$ becomes:

$$y(t) = k_2\left[\frac{4}{\pi}\sin(2\pi ft)\right]^2 + k_4\left[\frac{4}{\pi}(\sin(2\pi ft))\right]^4 \quad (13)$$

$$y(t) = k_2\frac{16}{\pi^2}\left[\frac{1}{2} - \frac{1}{2}\cos(4\pi ft)\right] + k_4\frac{256}{\pi^4}\left[\frac{\cos 8\pi ft - 4\cos 4\pi ft + 3}{4}\right] \quad (14)$$

For a dc component of:

$$y_{dc} = 0.81k_2 + 1.9k_4 \quad (15)$$

This case is equivalent to a sinusoidal signal input with a factor of $4/\pi$. Table 1 summarizes the calculated DC component of the harvester for a sinusoidal and square input signal, while a UWB harvester up to 11 GHz bandwidth is considered. In reality to estimate the harvested power when the signal is at low frequencies, we need to consider a maximum components order. The error is still negligible with the consideration of the 5th component. Table 1 shows clearly that the harvested power is almost two times higher when square signal is used. The k_4 coefficient effect is important as well as k_2 and can be predominant.

Table 1. Calculated dc components.

Input signal	Harmonics	Calculated dc components
Sinusoidal (5)	1	$y_{dc} = 0.50k_2 + 0.37k_4$
Square (< 2.2 GHz) (9)	5	$y_{dc} = 0.93k_2 + 1.24k_4$
Square (2.2 to 3.66 GHz) (11)	3	$y_{dc} = 0.81k_2 + 0.64k_4$
Square (> 3.66 GHz) (13), (14)	1	$y_{dc} = 0.81k_2 + 1.9k_4$

3. DESIGN CONSIDERATION

The rectifier design is a trade-off between several design performance requirements, including operating frequency, bandwidth, sensitivity, dynamic range, and temperature extremes. The diode's high input impedance complicates the network matching of the power detectors/harvesters over a wide band while maintaining its sensitivity. In high frequencies systems, this becomes more complex because we have to consider the package capacitance and inductance effects, the diode ohmic contact resistance, and the junction capacity and resistance.

In this section, a multi-stage RF power harvester based on a zero bias Schottky diode is designed. The UWB power harvester is designed with commercial software (ADS) using SKYWORKS SMS7630/079 diodes [20] to have best performance in terms of bandwidth and efficiency.

3.1. Diode Model

In order to achieve a better performance of the UWB power harvesting/transfer circuit, the characterization of the used diode is mandatory. The SPICE model of Schottky diode is provided by the manufacturer which used to perform the simulations under ADS software. As illustrated in the inset of Fig. 4, the measurement plane brings back to the diode level using a Through-Reflected-

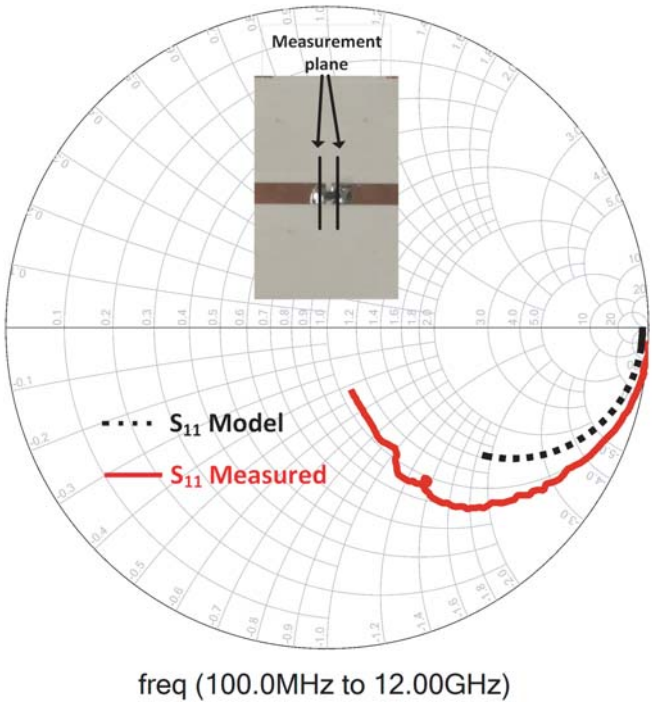

Figure 4. Diode model characterization.

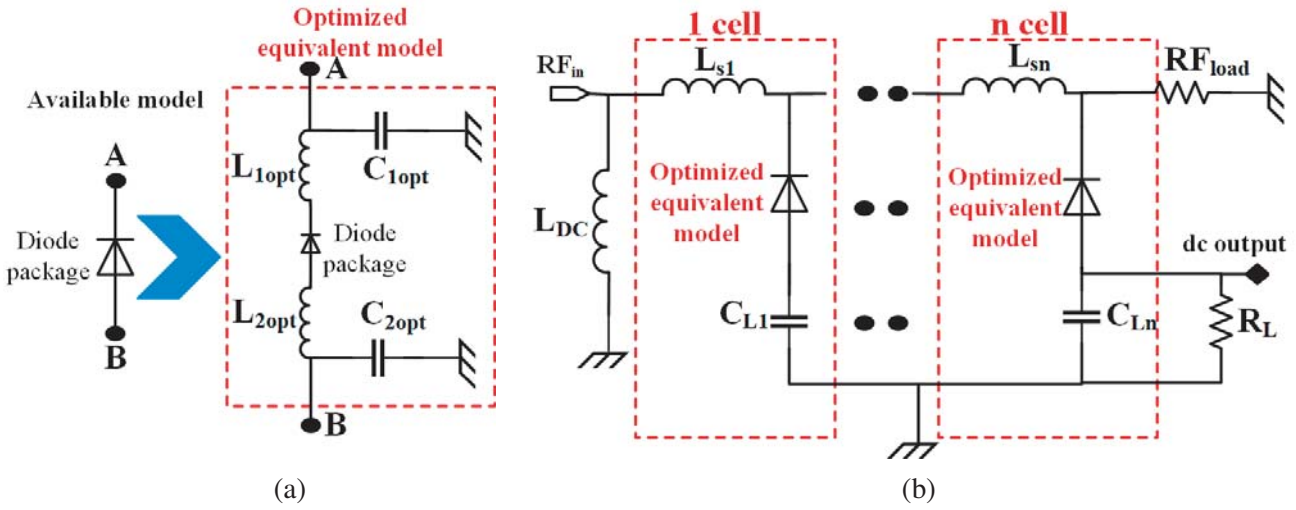

Figure 5. Power harvester circuit. (a) Optimized equivalent diode model (with $L_{1opt} = L_{2opt} = 0.6\,\text{nH}$ and $C_{1opt} = C_{2opt} = 0.04\,\text{pF}$) and (b) multistage configuration with $L_{DC} = 50\,\text{nH}$, $C_{Ln} = C_{L1} = 120\,\text{pF}$, $\text{RF}_{Load} = 120\,\Omega$ and $R_L = 100\,\Omega$ optimized for five stage circuit.

Line (TRL) kit manufactured for this purpose. As can be seen in Fig. 4, the measured reflection coefficient is different from that provided by the manufacturer, and this offset is probably due to the diode packaging effects. The experimental result shows more dispersive and reflective device-under-test (DUT). The measurement-based model will be used in next steps of the design including the lumped element components package model (Fig. 5(a)). Using ADS software, the optimized equivalent model of the diode shown in Fig. 5(a) is obtained by combining the measured parameters and those provided by the manufacturer (spice model and S-parameters).

3.2. Cell Number and RF_{load} Effect

Figure 5(b) shows the multi-stages power harvester configuration including a serials inductance. The diode has a very high input impedance. Therefore, increasing number of parallel cells reduces the total impedance of the device, and adding serials inductance reduces the capacitive effect of the diodes. As a result, reducing the power harvester input impedance facilitates the impedance matching. These inductances will be realized by high impedance microstrip lines (MSLs).

The resultant impedance is a critical parameter for the distributed harvester design. This ensures the maximization of power transfer from source to the harvester and a better matching of the dc output voltage. Thanks to the distributed elements, the harvester obtained a good performance over a wide range of input frequencies. Since the RF load resistor plays an essential role to short-circuit the RF return losses, it must be set to an optimal value to guarantee a good compromise between bandwidth and system sensitivity.

The simulated RF_{load} effect on the reflection coefficient denoted by S_{11} and the efficiency is depicted in Fig. 6. To observe the effect of the RF_{load} value on the performance of the power harvester, Fig. 6 illustrates the simulation results of the reflection coefficient and efficiency for different RF_{load} values. It should be noted that a trade-off is required between a better input matching and maximum efficiency over the whole bandwidth. The value of RF_{load} that best meets these requirements is $120\,\Omega$.

The number of stages effect is determined with respect to harvester efficiency as shown in Fig. 7. It can be seen that a 5-stage harvester is more efficient than a 9-stage one. Furthermore, a 5-stage harvester shows higher sensitivity, higher dynamic range, and larger power range. The number of stages selected is a matter of compromise with maximum efficiency and operating bandwidth of the power harvester.

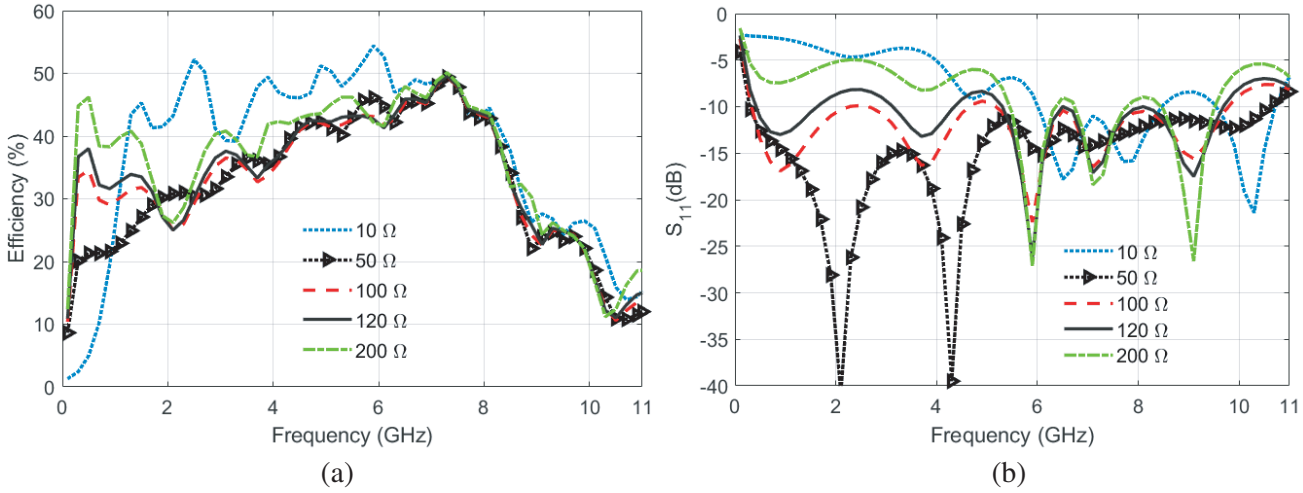

Figure 6. RF_{load} effect on reflection coefficient and efficiency of the power harvester.

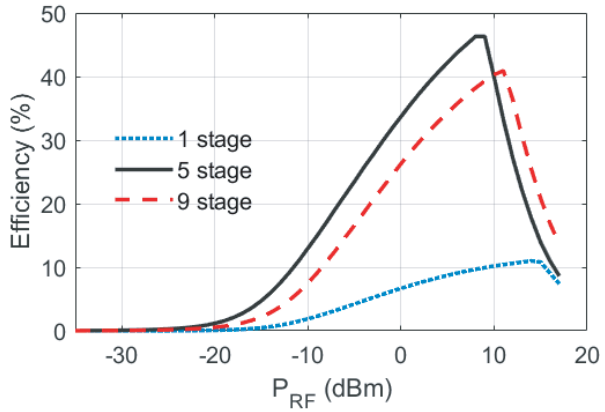

Figure 7. Number of cell effect on the power harvester efficiency.

3.3. Validation Results

A photograph of the fabricated circuit is shown in Fig. 8. A Rogers RT/duroid 6002 substrate with 0.762 mm of thickness is used. Fig. 9 shows the power harvester reflection coefficient at the operating

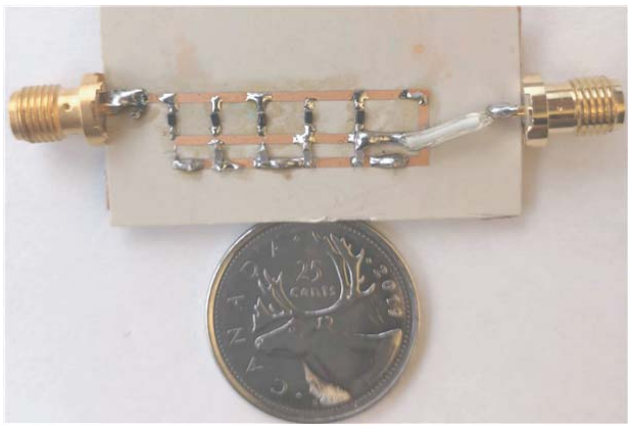

Figure 8. Photograph of the fabricated prototype.

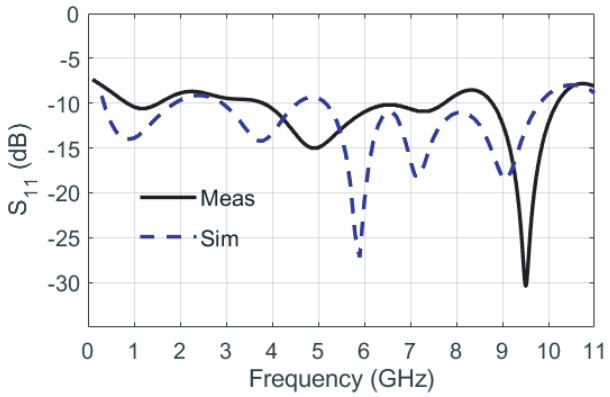

Figure 9. Measured and simulated results of reflection coefficient.

band with good agreement between the measured and simulated results. Standard calibration is used for the experimental characterization. A reflection coefficient of −10 dB is obtained over the expected 11 GHz of bandwidth, ranging from 100 MHz to 10 GHz (acceptable −8 dB is observed at 11 GHz). There is a slight difference between simulated and measured results due to the manufacturing process.

3.4. Sinusoidal Single Tone Signal Measurement

Figure 10 shows the dc output voltage versus the input power of the distributed power harvester for different frequencies in the operating bandwidth. A 3-D representation of the simulation and measurement results is chosen in order to provide a better view of the designed power harvester performance over the frequency bandwidth. The simulation results presented in Fig. 10(a) show a same behavior against the input power over the operating band of the harvester. Corresponding measured results are depicted in Fig. 10(b), which are in a good agreement with those simulated. The same level of saturation is observed with an increasing dropping with frequency.

The measured and simulated efficiencies are plotted as a function of input power in Fig. 11. A maximum power conversion efficiency of 48% is measured at 6 GHz for an input power from −40 to 17 dBm. It can be observed that the efficiency increases with input frequency (from 40% to 45%). The

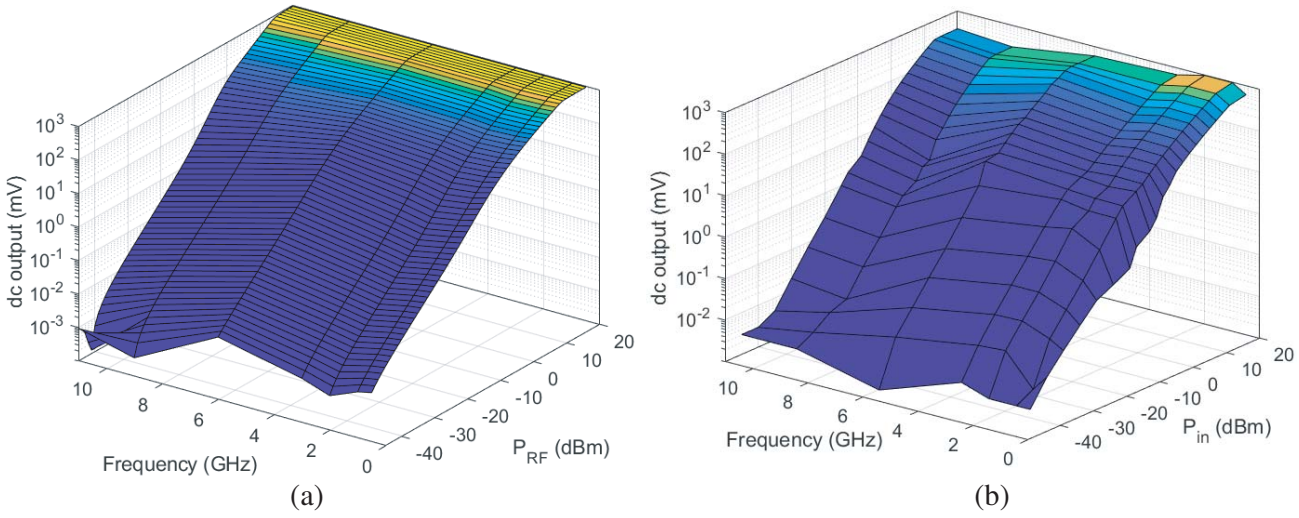

Figure 10. RF power versus dc output at different UWB frequencies. (a) Simulated results and (b) measured results.

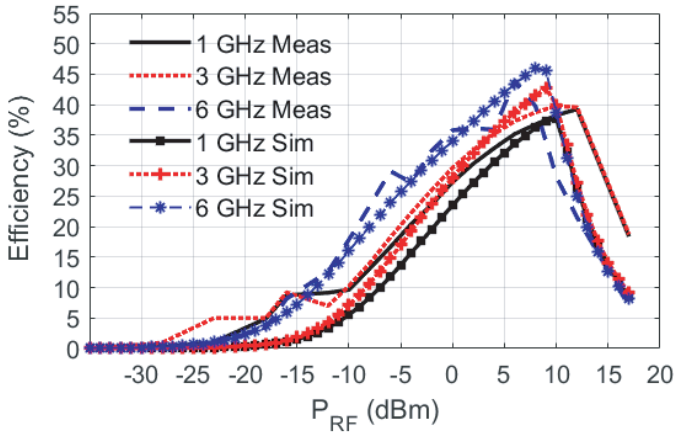

Figure 11. Measured and simulated efficiency.

power conversion efficiency is calculated according to Eq. (16).

$$\eta = \frac{P_{outdc}}{P_{in}} = \frac{V_{out}^2}{R_L P_{in}} \tag{16}$$

Table 2 summarizes some of the work carried out for RF power harvesting in the case multi-band and ultra-wide band with one single tone as reference. It is important to note that in the few works that cover UWB signal rectification, the operating band is often less than the spectrum allocated for UWB systems which ranges from 3 to 11 GHz.

Table 2. Power harvesting state of the art.

	Frequency (GHz)	Rectifier component	Efficiency Input power
[6]	Single 2.45	HSMS282C	60% at 13 dBm
[8]	Duel-band 0.915, 1.8	GaAs pHEMT + Avago HSMS2850	55%, 48% at 5 dBm
[3]	Triple-band 1.85, 2.18, 2.45	Avago HSMS2850	48%, 51%, 45% at −5 dBm
[7]	C-band 5.1-5.8	GaN Diode	30% at 38 dBm
[15]	Ultra-Wide-band 0.6–3	Skyworks SMS7630	46–66% at 17 dBm
This work	Ultra-Wide-band **0.1 – 11**	Skyworks SMS7630	40–45% at 8 dBm

4. PULSED SIGNAL MEASUREMENT

The proposed multistage rectifier design offers a broad band operating with maximum efficiency. The UWB power transfer requires a broad band RF power harvesting device to allow maximum power transmission to the load and can be used to rectify signal with large spectrum such as pulsed one with different shapes. Pulse Width Modulation (PWM), or Pulse Duration Modulation (PDM), is a method

of reducing the average power delivered by an electrical signal by efficiently cutting out it into discrete parts. In addition to the amplitude, a PWM signal behavior is defined by two main parameters: a) duty cycle (power cycle) and b) frequency [21, 22].

The rectification concept used for the UWB power transfer measurements is illustrated in Fig. 12. This idea is used in different IC like in PLL to convert the error signal efficiently from the charge pump to dc control voltage. The signal generator provides a controlled pulse in terms of width (duty cycle), period (frequency), and amplitude. Furthermore, the power transfer is done through the proposed five-stage power collector circuit. A low-pass filter (LPF) is added to the UWB five-stage rectifier to attenuate the high frequency signals generally associated with the carrier or noise. The simplest LPF is the passive RC circuit. The used first order LPF has only one reactive component. The parameters that define the filter are the cutoff frequency and the time constant which represents the capacitor charging duration of the final value of the steady state [23].

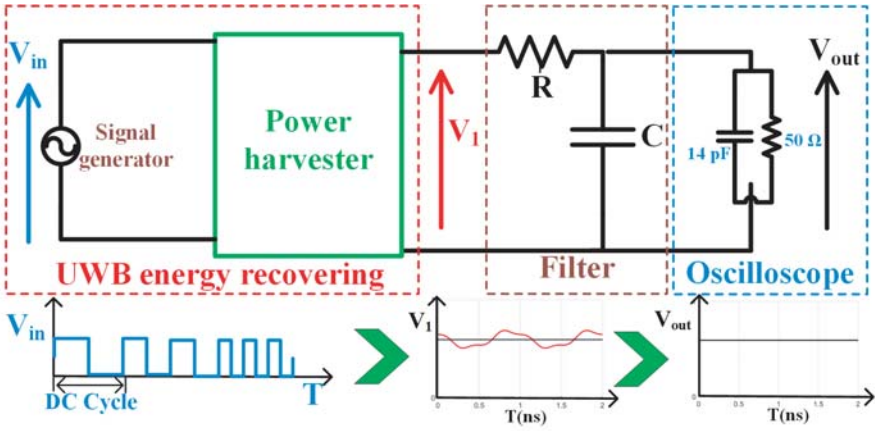

Figure 12. Block diagram of pulse power harvesting with $R = 1\,\mathrm{k\Omega}$ and $C = 5\,\mathrm{nF}$.

Figure 13 shows the measured signal waveform from the used Agilent 81133A pulse/pattern generator. It should be noted that the pulse provided by the generator is limited to 3 GHz with a maximum amplitude of 2 V, and its shape begins to degrade around 2 GHz. The measured circuit output versus input frequency is depicted in Fig. 14(a). In order to show better performances, the results are taken for a different level input signal from 0.1 to 2 V. We can see that our circuit can recover 99% of the input pulse voltage with amplitudes of 0.5 V and more. This efficiency is maintained for all frequencies

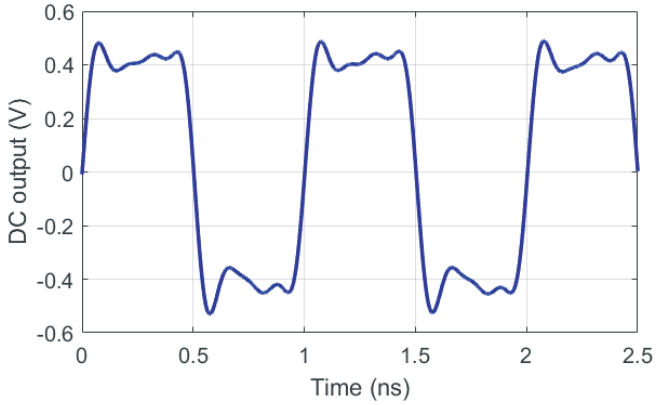

Figure 13. Measured generated signal from Agilent 81133A signal generator with 1 V of amplitude and 50% of duty cycle.

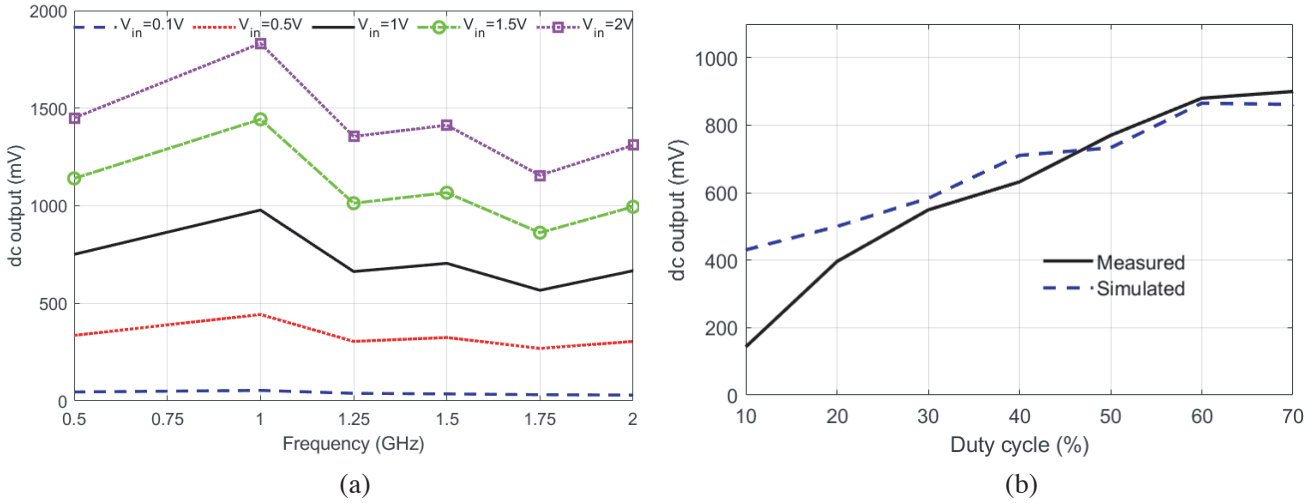

Figure 14. (a) Measured dc output with pulse as input signal and (b) measured and simulated dc output versus duty cycle at 2 GHz and 1 V of amplitude.

included in the harvester operating band. At frequency lower than 1 GHz, 11 harmonics are rectified by the five-stage circuit. Moreover, when the pulse contains more harmonics (desired or undesired), the dc output increases. It may be noted that the dc output voltage increases with frequency, seen in Equation (9).

Figure 14(b) illustrates the measured and simulated results of output signal versus duty cycle at 2 GHz of frequency and 1 V of input pulse amplitude. A good correspondence is noted between simulated and measured results, and the dc output is proportional to the duty cycle. As we can see, the dc output voltage increases proportionally with the duty cycle for a peak of 60%, and thereafter it saturates. Thus, it can be seen that the efficiency is better for a duty cycle ratio between 25% and 70% of the input signal period. It means that the wider the pulse width is, the more the power is transmitted. It can be noted that the minor difference between the measurement and simulation results comes from the pulse generator and the ripples at the high level of the pulse which cause unwanted harmonics at the dc output.

To test our circuit in a real environment, Fig. 15(a) shows the dedicated measurement setup. For transmission, a signal generator is used to generate the transmitted signal (Sine and Pulse) fed to a UWB antenna. At the reception, the power harvester is associated with an antenna similar to that of the transmission to collect the transmitted power, and to measure the dc voltage a digital multimeter is used. Two types of signals used in this work (sinusoidal and square) were sent with the same frequency

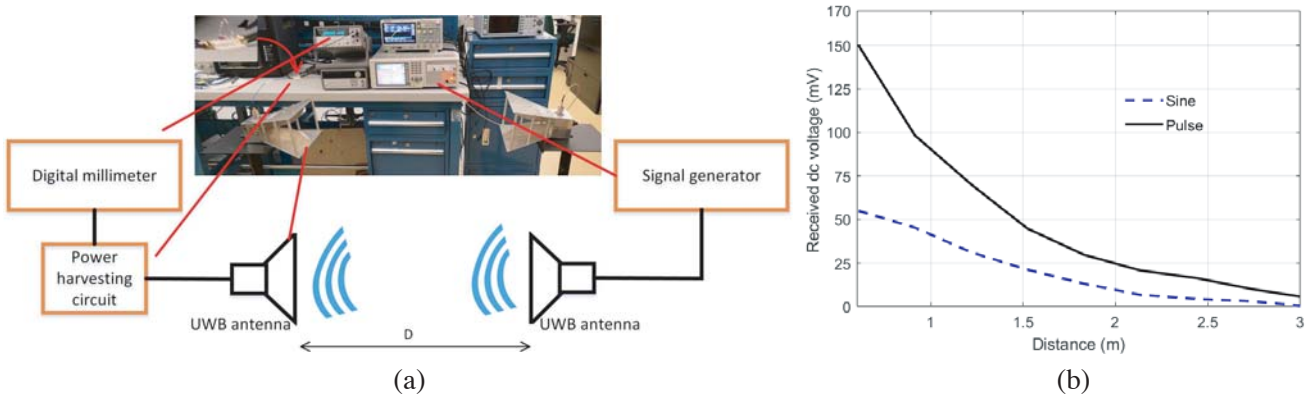

Figure 15. (a) UWB power harvesting/transfer setup and (b) received dc voltage.

(2 GHz) and same amplitude (1 V). For distances from 2 to 10 feet (0.6 to 3 m), the measured dc voltage is depicted in Fig. 15(b). It can be seen that for the same distance, the dc voltage measured in the case of a square wave signal is clearly higher (3 times) than that of the sinusoidal signal. This confirms the benefit of using a square wave signal (pulse) in the case of power harvesting or transfer.

5. CONCLUSION

An enhanced ultra-wide band five-stage rectifier for pulsed signal wireless power transfer is presented in this paper. The characterization of the diode model provides better performance in terms of efficiency and dynamic range. A broadband impedance matching network technique has been illustrated to achieve the matching requirement over 0.1–11 GHz bandwidth. The signal detection measurements proves the good performance of the design where the power harvester is measured at different UWB frequencies. The proposed rectifier circuit makes it possible to rectify a square wave signal with a low power spectral density and a different duty cycle. Furthermore, this rectifier offers more efficient control of the dc output by controlling the duty cycle or the input signal frequency as well as the amplitude. The far field measurement setup shows that the power transfer using square signal input can be 3 times more efficient than the sinusoidal one. In the future, a better combination of several signals with harmonics control and the design of a UWB antenna are planned in order to optimize the power harvesting/transfer system.

ACKNOWLEDGMENT

The author wishes to thank the Natural Sciences and Engineering Research Council of Canada (NSERC) and the Fonds Quebecois de la Recherche sur la Nature et les Technologies (FQNRT).

REFERENCES

1. Din, N. M., C. K. Chakrabarty, A. Bin Ismail, K. K. Devi, and W.-Y. Chen, "Design of RF energy harvesting system for energizing low power devices," *Progress In Electromagnetics Research*, Vol. 132, 49–69, 2012.
2. El Badawe, M. and O. M. Ramahi, "Efficient metasurface rectenna for electromagnetic wireless power transfer and energy harvesting," *Progress In Electromagnetics Research*, Vol. 161, 35–40, 2018.
3. Shen, S., Y. Zhang, C. Chiu, and R. Murch, "A triple-band high-gain multibeam ambient RF energy harvesting system utilizing hybrid combining," *IEEE Transactions on Industrial Electronics*, Vol. 67, No. 11, 9215–9226, 2020.
4. Du, Z. and X. Y. Zhang, "High-efficiency single- and dual-band rectifiers using a complex impedance compression network for wireless power transfer," *IEEE Transactions on Industrial Electronics*, Vol. 65, No. 6, 5012–5022, 2018.
5. Donelli, M., P. Rocca, and F. Viani, "Design of a WPT system for the powering of wireless sensor nodes: Theoretical guidelines and experimental validation," *Wireless Power Transfer*, Vol. 3, No. 1, 15–23, 2016.
6. Liu, C., F. Tan, H. Zhang, and Q. He, "A novel single-diode microwave rectifier with a series band-stop structure," *IEEE Transactions on Microwave Theory and Techniques*, Vol. 65, No. 2, 600–606, 2017.
7. Kawasaki, S., K. Ryoko, F. Yuki, N. Toshihiro, Y. Satoshi, N. Kenjiro, and S. Harunobu, "C-band energy harvester by Si RFICs with GaN diodes for microwave power transfer," *2017 IEEE International Symposium on Radio-Frequency Integration Technology, RFIT 2017*, 147–149, Seoul, South Korea, 2017.
8. Liu, Z., Z. Zhong, and Y. X. Guo, "Enhanced dual-band ambient RF energy harvesting with ultra-wide power range," *IEEE Microwave and Wireless Components Letters*, Vol. 25, No. 9, 630–632, 2015.

9. Niotaki, K., A. Georgiadis, and A. Collado, "Dual-band rectifier based on resistance compression networks," *IEEE MTT-S International Microwave Symposium Digest*, Vol. 1, 1–3, IEEE, Tampa, FL, USA, 2014.
10. Shariati, N., J. R. Scott, D. Schreurs, and K. Ghorbani, "Multitone excitation analysis in RF energy harvesters-considerations and limitations," *IEEE Internet of Things Journal*, Vol. 5, No. 4, 2804–2816, 2018.
11. Zeng, Y., B. Clerckx, and R. Zhang, "Communications and signals design for wireless power transmission," *IEEE Transactions on Communications*, Vol. 65, No. 5, 2264–2290, 2017.
12. Henning, F. H., *Transmission of Information by Orthogonal Functions*, Vol. 87, No. 4, Springer, 2012.
13. Ross, G. F. and M. Lexington, "Transmission and reception system for generating and receiving base-band duration pulse signals for short base-band pulse communication system," 912–914, 1973.
14. Albreem, M. A., "5G wireless communication systems: Vision and challenges," *I4CT 2015 — 2015 2nd International Conference on Computer, Communications, and Control Technology, Art Proceeding*, No. I4ct, 493–497, IEEE, Kuching, Sarawak, Malaysia, 2015.
15. Zheng, S., W. Liu, and Y. Pan, "Design of an ultra-wideband high-efficiency rectifier for wireless power transmission and harvesting applications," *IEEE Transactions on Industrial Informatics*, Vol. 15, No. 6, 3334–3342, 2019.
16. Moulay, A. and T. Djerafi, "Multi-stage schottky diode power harvester for UWB application," *IEEE Wireless Power Transfer Conference (WPTC)*, 8–11, Montreal, Canada, 2018.
17. Boaventura, A. S. and N. B. Carvalho, "Maximizing DC power in energy harvesting circuits using multisine excitation," *IEEE MTT-S International Microwave Symposium Digest*, Vol. 1, No. 1, 1–4, Baltimore, MD, USA, 2011.
18. Bahl, I. J., *Fundamentals of RF and Microwave Transistor Amplifiers*, John Wiley & Sons, Hoboken, New Jersey, 2009.
19. Jose Carlos, P. and N. B. Carvalho, *Intermodulation Distortion in Microwave and Wireless Circuits*, Artech House, 2003.
20. Skyworks, "SM76XX Datasheet. Surface mount mixer and detector Schottky diodes," *Tech. Rep.*, Skyworks, 2015.
21. Yang, Y. L., C. L. Tsai, C. W. Yang, and C. L. Yang, "Using pulse width and waveform modulation to enhance power conversion efficiency under constraint of low input power," *Asia-Pacific Microwave Conference Proceedings*, 400–402, APMC, 2012.
22. Metivier, R., "Method for converting a PWM output to an analog output when using hall-effect sensor ICs," *Allegro MicroSystems*, No. 296094-AN, 2013.
23. Sinar, D. and G. Knopf, "Printed graphene derivative circuits as passive electrical filters," *Nanomaterials*, Vol. 8, No. 2, 123, 2018.